DESY 17-104

arXiv:1708.04650v1 [hep-ph] 15 Aug 2017

A New Look at the Y Tetraquarks and Ω_c Baryons in the Diquark Model

Ahmed Ali,[1,*] Luciano Maiani,[2,†] Anatoly V. Borisov,[3,‡] Ishtiaq Ahmed,[4,§] M. Jamil Aslam,[5,¶] Alexander Ya. Parkhomenko,[6,**] Antonio D. Polosa,[7,††] and Abdur Rehman[4,‡‡]

[1]*Deutsches Elektronen-Synchrotron DESY, D-22607 Hamburg, Germany*
[2]*Theory Division, CERN, Geneva, Switzerland*
[3]*Faculty of Physics, Moscow State University, 119991 Moscow, Russia*
[4]*National Centre for Physics, Quaid-i-Azam University Campus, Islamabad, 45320, Pakistan*
[5]*Department of Physics, Quaid-i-Azam University, Islamabad, 45320, Pakistan*
[6]*Department of Theoretical Physics, P. G. Demidov Yaroslavl State University, Sovietskaya 14, 150003 Yaroslavl, Russia*
[7]*Dipartimento di Fisica and INFN, Sapienza Universita di Roma, Piazzale Aldo Moro 2, I-00185 Roma, Italy*

(Dated: August 17, 2017)

We analyze the hidden charm P-wave tetraquarks in the diquark model, using an effective Hamiltonian incorporating the dominant spin-spin, spin-orbit and tensor interactions, comparing with the P-wave charmonia and with the recent analysis of the newly discovered Ω_c baryons. Given the uncertain experimental situation on the Y states, we allow for two different spectra and discuss the related parameters in the diquark model, including the constrains from Ω_c baryons. The diquark model allows to select a preferable Y-states pattern. The existence of higher resonances, as the one predicted with $L = 3$, would be another footprint of the underlying diquark dynamics.

PACS numbers:

I. INTRODUCTION

The experimental discovery of the four-quark (more precisely two quarks and two antiquarks) and five-quark (four quarks and an antiquark) states has opened a new field in hadron spectroscopy. The exotic four- and five-quark states, called X, Y, Z and P_c, respectively, have been analyzed in a number of theoretical models, reviewed recently in [1–4]. We will concentrate on the diquark-antidiquark interpretation that, for heavy-light diquarks, was introduced in [5] for hidden charm and in [6] for hidden beauty, following the light pentaquark picture discussed in [7].

The objects of our interest in this note are the $J^{PC} = 1^{--}$ states, the so called Y-resonances. In [8], the four basic $L = 1$ resonances with, $J^{PC} = 1^{--}$ in the diquark-antidiquark spectrum were identified with $Y(4008)$, $Y(4260)$, $Y(4290)$ (a broad structure in the h_c channel), or $Y(4220)$ (a narrow structure) and $Y(4630)$.

Since that paper appeared, the experimental situation has evolved. The assessment of the $Y(4008)$ is under review and the $Y(4260)$, which apparently was the best established resonance, is now claimed by BESIII as a double humped structure [9]. The $Y(4360)$ and $Y(4660)$ were considered to be $n = 2$ radial excitations of $Y(4008)$ and $Y(4260)$, respectively, motivated by their decays into $\psi(2S)\pi^+\pi^-$, and the mass differences, which are similar to the ones in the radial excitations of the quarkonium states, $\chi_{(c,b),J}(2P) - \chi_{(c,b),J}(1P)$. On the other hand, it was also observed that $Y(4630)$ and $Y(4660)$ could be fitted as a unique resonance, mainly decaying into $\Lambda\bar{\Lambda}$ [10].

Given the experimental uncertainties that still affect this sector, we shall work out our analysis on two distinct spectra, based essentially on the Belle and BaBar data, and on the more recent BESIII data, respectively, which we define as scenario I and II, (namely SI and SII). The main distinction between SI and SII is that the first one contains the $Y(4008)$ and the other does not. In both SI and SII we shall keep $Y(4660)$ and $Y(4630)$ to correspond to the same state. In SI we include

$$\text{SI}: \quad \text{Y(4008)}, \text{Y(4260)}, \text{Y(4360)}, \text{Y(4660)},$$

whereas in SII we have

$$\text{SII}: \quad Y(4220), Y(4330), Y(4390), Y(4660).$$

Thus, in SI, we include the $Y(4360)$, which was previously considered a radial excitation, whereas in SII, the spectrum starts with $Y(4220)$, *i.e.*, the narrow structure mentioned above with reference to [8]. In SII, $Y(4330)$ and $Y(4390)$ correspond to the two lines resolving the $Y(4260)$, according to BESIII [9]. The $Y(4008)$ has been seen so far by Belle only [11], about 250 MeV below the well-established $Y(4260)$. Current analysis of this resonance from BESIII is inconclusive [9].

In calculating the mass spectrum, tensor coupling interactions were not included in [8]. Here we take a second look at the four Y-states, in both SI and SII, treating them as $n = 1$ P-states, with the mass differences

*Electronic address: ahmed.ali@desy.de
†Electronic address: Luciano.Maiani@cern.ch
‡Electronic address: borisov@phys.msu.ru
§Electronic address: ishtiaqmusab@gmail.com
¶Electronic address: muhammadjamil.aslam@gmail.com
**Electronic address: parkh@uniyar.ac.ru
††Electronic address: antonio.polosa@roma1.infn.it
‡‡Electronic address: Abdur.Rehman@fuw.edu.pl

accounted for by the spin-orbit, spin-spin and tensor interactions.

The Y-states have also been interpreted as hadron molecules in [12], though $Y(4008)$ is not foreseen in that case. The state $Y(4260)$ has also been advocated as an example of a $(c\bar{c})_8 g$ hybrid [13]. However, due to the recent evidence that $Y(4260)$ decays into $h_c\pi^+\pi^-$ [14] — a heavy quark spin- flip transition — this interpretation is now disfavored. Another analysis of Y states in the diquark approach can be found in [15].

Closely related to the analysis of tetraquark Y-states, presented here, are the five narrow excited charmed-baryon states $\Omega_c(=css)$, whose mass spectrum has recently been measured by the LHCb collaboration [16].

Following [17], we treat them as diquark-quark systems, $[ss]c$ (for the Ω_c-baryons) with the $[ss]$-diquark having the spin $S_{[ss]}=1$.

The five Ω_c states are assumed to have orbital angular momentum $L=1$. Their measured masses (in MeV) [16], and the assumed J^P-quantum numbers are as follows:

$$\begin{aligned} M(\Omega_c(3000)) &= 3000.4\pm0.2\pm0.1;\ J^P=1/2^-, \\ M(\Omega_c(3050)) &= 3050.2\pm0.1\pm0.1;\ J^P=1/2^-, \\ M(\Omega_c(3066)) &= 3065.6\pm0.1\pm0.3;\ J^P=3/2^-, \quad (1)\\ M(\Omega_c(3090)) &= 3090.2\pm0.3\pm0.5;\ J^P=3/2^-, \\ M(\Omega_c(3119)) &= 3119.1\pm0.3\pm0.9;\ J^P=5/2^-. \end{aligned}$$

With the spin of the c-quark being $S_c=1/2$, we have total spin $S=1/2$ or $3/2$. Combined with the orbital angular momentum $L=1$ yields the five observed Ω_c states, having $J=1/2$ (two states), $J=3/2$ (two states), and $J=5/2$ (one state). They have been discussed in a number of papers [17–20]. We follow here the analysis by Karliner and Rosner [17], where the effects of the tensor contribution have been implemented, in addition to the spin-spin and spin-orbit terms in calculating the mass spectrum.

The principal aim of this paper is to investigate whether the diquark picture provides a satisfactory description of the four Y-states in the $c\bar{c}$ sector, effectively distinguishing between SI and SII. In doing so, we first repeat the analysis of the five $L=1$ charmed-baryons Ω_c.

II. EFFECTIVE HAMILTONIAN FOR THE Ω_c BARYONS

In the diquark-quark description, the Hamiltonian for the Ω_c states can be written as

$$\begin{aligned} H_{\text{eff}} &= m_c + m_{[ss]} + \kappa_{ss}\boldsymbol{S}_s\cdot\boldsymbol{S}_s + \frac{B_{\mathcal{Q}}}{2}\boldsymbol{L}^2 + V_{SD}, \quad (2)\\ V_{SD} &= a_1\boldsymbol{L}\cdot\boldsymbol{S}_{[ss]} + a_2\boldsymbol{L}\cdot\boldsymbol{S}_c + b\frac{\langle S_{12}\rangle}{4} + c\,\boldsymbol{S}_{[ss]}\cdot\boldsymbol{S}_c. \end{aligned}$$

In Eq. (2), m_c and $m_{[ss]}$ are the masses of the c quark and the $[ss]$ diquark, respectively, κ_{ss} is the spin-spin coupling of the quarks in the diquark, and $\boldsymbol{L}$ is the orbital angular momentum of the diquark-quark system. The spin-dependent part of the Hamiltonian V_{SD} is taken from [17]. The coefficients a_1 and a_2 are the strengths of the spin-orbit terms involving the spin of the diquark $\boldsymbol{S}_{[ss]}$ and the charm-quark spin $\boldsymbol{S}_c$, respectively. The term $b\langle S_{12}\rangle/4$ represents the matrix element of the tensor interaction, defined by

$$\frac{S_{12}}{4} = Q(\boldsymbol{S}_1,\boldsymbol{S}_2) = 3(\boldsymbol{S}_1\cdot\boldsymbol{n})(\boldsymbol{S}_2\cdot\boldsymbol{n}) - (\boldsymbol{S}_1\cdot\boldsymbol{S}_2), \quad (3)$$

where $\boldsymbol{S}_1$ and $\boldsymbol{S}_2$ are the spins of the diquark and the charm quark, respectively, and $\boldsymbol{n}=\boldsymbol{r}/r$ is the unit vector along the radius vector of a particle. This notation is used in the analysis of the $L=1$ Y-states as well, in which case $\boldsymbol{S}_2$ represents the spin of the antidiquark.

The scalar operator of Eq. (3) can be expressed as the convolution $3S_1^iS_2^jN_{ij}$, where the tensor operator

$$N_{ij} = n_in_j - \frac{1}{3}\delta_{ij}. \quad (4)$$

For further applications, we need the matrix elements of this operator between the states with the same fixed value L of the angular momentum operator $\boldsymbol{L}$, using an identity from Landau and Lifshitz [22]:

$$\langle N_{ij}\rangle = a(L)(L_iL_j + L_jL_i - \frac{2}{3}\delta_{ij}L(L+1)), \quad (5)$$

where $a(L)=\frac{-1}{(2L-1)(2L+3)}$.

Saturating the operator inside the brackets of Eq. (5) with the product of the spin operators $S_X^iS_X^j$, with $\boldsymbol{S}_X=\boldsymbol{S}_c,\boldsymbol{S}_d$ and $\boldsymbol{S}$, which are the spins of the c quark, $d=[ss]$ diquark and the total spin of the system, respectively, using the appropriate commutation relations of the components of $\boldsymbol{S}_X$, and setting $L=1$, one finds easily (see e.g. the Appendix of [17]):

$$\langle Q(\boldsymbol{S}_X,\boldsymbol{S}_X)\rangle = -\frac{3}{5}\langle[2(\boldsymbol{L}\cdot\boldsymbol{S}_X)^2 + (\boldsymbol{L}\cdot\boldsymbol{S}_X) - \frac{4}{3}(\boldsymbol{S}_X\cdot\boldsymbol{S}_X)]\rangle. \quad (6)$$

For spin 1/2 values of $S_{1,2}$, the second and third terms in (6) do vanish and one recovers the usual formula for the tensor coupling used for the P-wave charmonia (see, e.g., [23]). In terms of the $Q(\boldsymbol{S}_X,\boldsymbol{S}_X)$, Eq. (3) for the present case can be expressed as

$$\frac{\langle S_{12}\rangle}{2} = \langle 2Q(\boldsymbol{S}_d,\boldsymbol{S}_c)\rangle = \langle Q(\boldsymbol{S},\boldsymbol{S}) - Q(\boldsymbol{S}_c,\boldsymbol{S}_c) - Q(\boldsymbol{S}_d,\boldsymbol{S}_d)\rangle. \quad (7)$$

In particular, if $\boldsymbol{S}_X=\boldsymbol{S}_{[ss]},\boldsymbol{S}_c$, we are interested in the matrix elements

$$\langle L,S';J|\boldsymbol{L}\cdot\boldsymbol{S}_X|L,S;J\rangle, \quad (8)$$

where $L=1$, the total angular momentum can be $J=1/2$, $3/2$ and the total spin is S, $S'=1/2$, $3/2$. For $J=5/2$, S is necessarily $3/2$.

The matrix elements can be computed directly by applying the operators $\boldsymbol{L}\cdot\boldsymbol{S}_X$ to the products of states corresponding to the individual angular momenta, $\boldsymbol{S}_{ss},\boldsymbol{S}_c,\boldsymbol{L}$.

TABLE I: Values of the parameters a_1, a_2, b, c and M_0 (in MeV), determined from the masses of the Ω_c baryons given in Eq. (1).

a_1	a_2	b	c	M_0
26.95	25.75	13.52	4.07	3079.94

More effectively, one can use Wigner's $6j$ symbols (now easily implemented in a computer code), as is customary for analogous cases in atomic and nuclear physics, and explained in the Appendix A.

In either way, one obtains:

$$\begin{aligned} J=1/2: \quad & \frac{1}{4}\langle S_{12}\rangle = \begin{pmatrix} 0 & \frac{1}{\sqrt{2}} \\ \frac{1}{\sqrt{2}} & -1 \end{pmatrix}, \\ J=3/2: \quad & \frac{1}{4}\langle S_{12}\rangle = \begin{pmatrix} 0 & -\frac{1}{2\sqrt{5}} \\ -\frac{1}{2\sqrt{5}} & \frac{4}{5} \end{pmatrix}, \\ J=5/2: \quad & \frac{1}{4}\langle S_{12}\rangle = -\frac{1}{5}. \end{aligned} \tag{9}$$

After diagonalizing the combined matrices of $\langle S_{12}\rangle$, given in Eq. (9), and that of $\boldsymbol{L}\cdot\boldsymbol{S}_{[ss],c}$ for the different J^P states, given in Appendix of [17] (c.f. Eq. (A12)–(A14)), we get the mass corrections arising due to these spin-orbit interactions. We remind that in all the five states, there is the common mass term $M_0 \equiv m_c + m_{[ss]} + 2\kappa_{ss} + B_{\mathcal{Q}}$.

In order to determine the parameters a_1, a_2, b and c, Karliner and Rosner [17] have used the spin averaged mass and have worked with the mass differences of the five Ω_c states. We reproduce their values, summarized in Table I, where we have also given the value of M_0.

III. EFFECTIVE HAMILTONIAN FOR Y TETRAQUARKS

Y-states have the quark content $[cq]_{\bar{3}}[\bar{c}\bar{q}]_3$, where the subscripts denote the color representations. Tetraquarks with $J^{PC}=1^{--}$ are obtained for $L=1$, 3. Spin wave functions are given in Table II, in the basis $\boldsymbol{S}_{\mathcal{Q}}$, $\boldsymbol{S}_{\bar{\mathcal{Q}}}$, $\boldsymbol{L}$ with $\boldsymbol{S}=\boldsymbol{S}_{\mathcal{Q}}+\boldsymbol{S}_{\bar{\mathcal{Q}}}$ and $\boldsymbol{J}=\boldsymbol{S}+\boldsymbol{L}$.

We extend the Hamiltonian of P-wave tetraquarks given in [8] by including the tensor coupling contribution

$$\begin{aligned} H_{\text{eff}} &= 2m_{\mathcal{Q}} + \frac{B_{\mathcal{Q}}}{2}\boldsymbol{L}^2 - 3\kappa_{cq} + 2a_Y \boldsymbol{L}\cdot\boldsymbol{S} + b_Y\frac{\langle S_{12}\rangle}{4} \\ &+ \kappa_{cq}\big[2(\boldsymbol{S_q}\cdot\boldsymbol{S_c} + \boldsymbol{S_{\bar{q}}}\cdot\boldsymbol{S_{\bar{c}}}) + 3\big], \end{aligned} \tag{10}$$

where S_{12} is defined as in (3) with $\boldsymbol{S}_{1,2}$ representing the spins of the two diquarks. Comparing to (2), we see that in this case the coefficients a_1 and a_2 are $a_1=a_2\equiv 2a_Y$ due to the charge conjugation invariance. The spin-spin interaction between diquark and antidiquark is neglected here since in P-wave the overlap probability is suppressed [8]. In the Ω_c case, the spin-spin interaction, represented by c, Table I, is similarly suppressed and the same happens in P-wave charmonia.

TABLE II: $J^{PC}=1^{--}$ tetraquarks involving a diquark-antidiquark $\mathcal{Q}\bar{\mathcal{Q}}$ pair in the diquark model.

Label	$\vert S_{\mathcal{Q}}, S_{\bar{\mathcal{Q}}}; S, L\rangle_J$
Y_1	$\vert 0,0;0,1\rangle_1$
Y_2	$\big(\vert 1,0;1,1\rangle_1 + \vert 0,1;1,1\rangle_1\big)/\sqrt{2}$
Y_3	$\vert 1,1;0,1\rangle_1$
Y_4	$\vert 1,1;2,1\rangle_1$
Y_5	$\vert 1,1;2,3\rangle_1$

The calculation of the matrix elements of the $\boldsymbol{L}\cdot\boldsymbol{S}_X$ operator, with $\boldsymbol{S}_X=\boldsymbol{S}_{[cq]}, \boldsymbol{S}_{[\bar{c}\bar{q}']}$ is described in the Appendix, Eq. (A24) and (A26). We note here that:

- tensor couplings are non vanishing only for the states with $S_{\mathcal{Q}}=S_{\bar{\mathcal{Q}}}=1$;
- the operator $\boldsymbol{L}\cdot\boldsymbol{S}_{\mathcal{Q}}$ is not invariant under the charge conjugation and it does mix the states Y_3 and Y_4, with a $J^{PC}=1^{-+}$ state of the spin composition:

$$Y^{(+)} = |1,1;1,1\rangle_1. \tag{11}$$

- $Y^{(+)}$ appears as an intermediate state in the product $(\boldsymbol{L}\cdot\boldsymbol{S}_{\mathcal{Q}})(\boldsymbol{L}\cdot\boldsymbol{S}_{\bar{\mathcal{Q}}})$, giving contribution to both the diagonal and the non diagonal terms to the matrix elements of the product between Y_3 and Y_4.

After Eqs. (A24), (A26), (7) and (10), tensor couplings over the $Y_3 - Y_4$ states are represented by the non-diagonal matrix:

$$\frac{1}{4}\langle S_{12}\rangle = \begin{pmatrix} 0 & 2/\sqrt{5} \\ 2/\sqrt{5} & -7/5 \end{pmatrix}. \tag{12}$$

The eigenvalues of the mass matrix of Y-states derived from Eqs. (10) and (12), are written as:

$$\begin{aligned} M_1 = M(Y_1) &= M_{00} - 3\kappa_{cq} \equiv \widetilde{M}_{00}, \\ M_2 = M(Y_2) &= \widetilde{M}_{00} - 2a_Y + 2\kappa_{cq}, \\ M_3 &= \widetilde{M}_{00} + 4\kappa_{cq} + E_+, \\ M_4 &= \widetilde{M}_{00} + 4\kappa_{cq} + E_-. \end{aligned} \tag{13}$$

We have made explicit that the states $Y_{1,2}$ in Table II are eigenstates of the mass matrix, while $M_{3,4}$ are the eigenvalues of the matrix

$$2a_Y\langle\boldsymbol{L}\cdot\boldsymbol{S}\rangle + b_Y\langle S_{12}\rangle/4, \tag{14}$$

with

$$E_{\pm} = \frac{1}{10} \times$$
$$\times \left(-30a_Y - 7b_Y \mp \sqrt{3}\sqrt{300a_Y^2 + 140a_Y b_Y + 43b_Y^2} \right),$$
$$M_3 + M_4 = 2(\widetilde{M}_{00} + 4\kappa_{cq}) + \frac{1}{5}(-30a_Y - 7b_Y)$$
$$= 2(\widetilde{M}_{00} + 4\kappa_{cq}) + E_+ + E_-,$$
$$M_4 - M_3 = \frac{\sqrt{3}}{5}\sqrt{300a_Y^2 + 140a_Y b_Y + 43b_Y^2}$$
$$= E_- - E_+ \geq 0. \quad (15)$$

We have also used: $M_{00} = 2m_Q + B_Q$.

In the hypothesis SI, we take the four $J^{PC} = 1^{--}$ Y-states to be $Y(4008)$, $Y(4260)$, $Y(4360)$ and $Y(4660)$, with masses (all in MeV)

$$M_1 = 4008 \pm 40^{+114}_{-28}, \quad M_2 = 4230 \pm 8,$$
$$M_3 = 4341 \pm 8, \quad M_4 = 4643 \pm 9. \quad (16)$$

Masses are taken from PDG [26], except for the $Y(4008)$, which is from Belle [11]. In their analysis, they find that their data are better fit with two resonances, $Y(4260)$ and $Y(4008)$, and the width of the $Y(4008)$ is found to be a factor 2 larger than that of the $Y(4260)$.

In the hypothesis SII, $Y(4008)$ is absent and the $Y(4260)$ is resolved in two peaks [27]. The masses of the states $Y(4220)$, $Y(4320)$, $Y(4390)$ and $Y(4660)$ are (all in MeV):

$$M_1 = 4219.6 \pm 3.3 \pm 5.1, \quad M_2 = 4333.2 \pm 19.9,$$
$$M_3 = 4391.5 \pm 6.3, \quad M_4 = 4643 \pm 9, \quad (17)$$

i.e. the state with the mass M_4 is the same as in SI.

Before proceeding to the estimate of the values of the parameters M_{00}, a_Y, κ_{cq} and b_Y, we first note their possible interdependence on each other. From Eq. (15) for $M_4 - M_3$ follows that this mass difference is invariant under the simultaneous sign change $(a_Y, b_Y) \to (-a_Y, -b_Y)$. Hence, from this mass difference alone, we have two solutions: $a_Y < 0$ and $a_Y > 0$. We shall call them case 1 and case 2, respectively. In line with the analysis for the Ω_c states, given in Table I, only $a_Y > 0$ should be kept. This is also the choice suggested by the mass ordering, in which the $L = 3$ state (called Y_5 in Table II) should have a higher mass than the $L = 1$ states. So, the only physically acceptable solution is the one which has positive value of a_Y irrespective of the sign of the value of b_Y.

However, as the experimental situation is currently not univocal, and the errors on some of the masses are large, we shall see below that, including the errors, solutions whose central values have $a_Y < 0$, are also allowed. In addition to Eq. (15), the mass difference $M_2 - M_1$ provides a constraint on the parameters a_Y and κ_{cq}:

$$M_2 - M_1 = 2(\kappa_{cq} - a_Y). \quad (18)$$

TABLE III: Values of the parameters in the Scenario I (SI) and II (SII) and $\pm 1\sigma$ errors (all in MeV). Here, $c1$ and $c2$ abbreviate the cases 1 and 2, respectively.

	a_Y	b_Y	κ_{cq}	M_{00}
SI (c1)	-22 ± 32	-89 ± 77	89 ± 11	4275 ± 54
SI (c2)	48 ± 23	11 ± 91	159 ± 20	4484 ± 26
SII (c1)	-3 ± 18	-105 ± 32	54 ± 8	4380 ± 25
SII (c2)	48 ± 8	-32 ± 47	105 ± 4	4535 ± 10

Thus, in both the scenarios for the Y_i masses, $\kappa_{cq} > a_Y$, with the two approaching each other as this mass difference decreases. The central values of the parameters a_Y, b_Y, κ_{cq}, and M_{00} are determined from the masses given in Eq. (16) for SI and in Eq. (17) for SII and presented in Table III.

To work out errors and the correlations among the parameters, we have used the method of least squares to determine the best-fit values and the covariance matrices. For this, the χ^2-function is calculated. In general [26],

$$\chi^2(\vec{\theta}) = \sum_{i=1}^{N} \frac{\left(y_i - \mu_i(\vec{\theta})\right)^2}{\Delta y_i^2}, \quad (19)$$

where $\vec{y} = (y_1, \ldots, y_N)$ is the set of the experimentally measured values which are assumed to be independent and Δy_i are their variances. The quantities $\mu_i(\vec{\theta})$ are dependent on the unknown parameters which are collected as the vector $\vec{\theta} = (\theta_1, \ldots, \theta_m)$ where $m \leq N$. For the problem at hand, we take the parameter-dependent functions from Eq. (13), $\mu_i(\vec{\theta}) = M_i$, where $i = 1, \cdots, 4$, and

$$\vec{\theta} = (\theta_1, \theta_2, \theta_3, \theta_4) \equiv (M_{00}, \kappa_{cq}, a_Y, b_Y). \quad (20)$$

The best-fit estimations of the parameters θ_k, obtained after minimizing the χ^2-function, are presented in Table III, as central values. Note that each scenario results into two solutions which differ by the sign of the best-fit value of a_Y, in line with the discussion above. The variances of the parameters are also shown in Table III, while the correlation matrices are collected in Appendix B. The parameters (20) are strongly correlated as all the correlation moments in the corresponding matrices (B1)–(B4) are close in magnitude to unity. To show this, we plot two-dimensional confidence level (C.L.) contours involving some of the coefficients.

The correlations among the parameters a_Y and b_Y and in terms of the 68.3% ($\chi^2 = \chi^2_{\min} + 2.3$ for two degrees of freedom) and 95.4% ($\chi^2 = \chi^2_{\min} + 6.18$) C.L. contours are presented in Fig. 1. Similar contours demonstrating correlations among a_Y and κ_{cq} are shown in Fig. 2. The first and the second rows in these figures correspond to the Scenario I and II, respectively, and in each row, the left panels are plotted for the negative best-fit value of a_Y (case 1), while the right panels are for the positive best-fit value (case 2). Our analysis shows that Scenario I

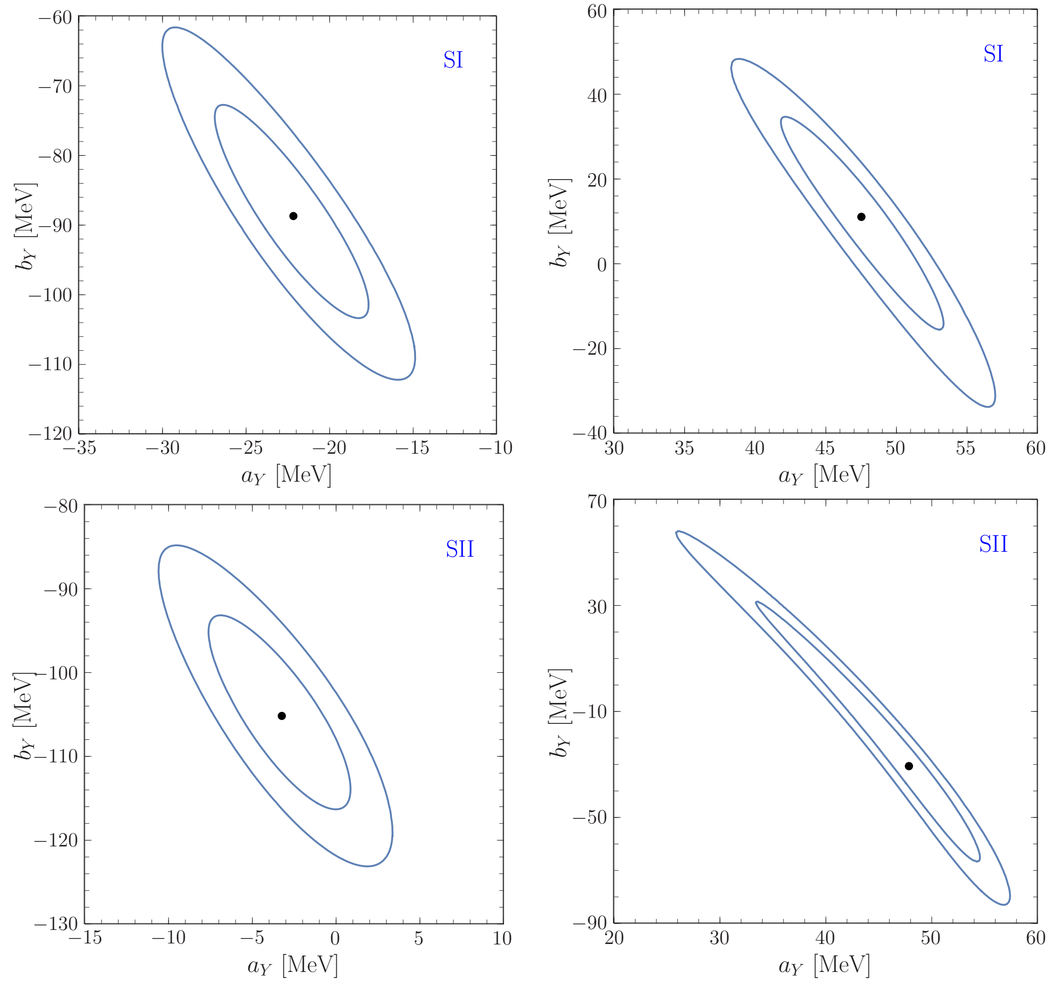

FIG. 1: 1σ- and 2σ-contours in the $a_Y - b_Y$ parameter plane corresponding to 68.3% and 95.4% C.L. for the scenario I (SI) in the top two frames and scenario II (SII) in the bottom two frames. The dot in each frame shows the position of the best-fit value which is the minimum of the χ^2-function. The best-fit value of a_Y is negative (case 1) in the left panels and positive (case 2) in the right panels.

(case 1) is not tenable, as, within 95.4% C.L. and even higher, a_Y remains negative. Thus, the requirement of positive a_Y disfavors case 1 in Scenario I. In Scenario II (case 1), small positive values of a_Y are allowed with a relatively large probability. In case 2, large positive values of a_Y are predicted for both Scenario I and II,

IV. DISCUSSION

With the current uncertainty of the experimental scenarios and many parameters one cannot draw quantitative conclusions, except observing that the values of the parameters are qualitatively similar to those derived in the P-wave Ω_c-states in three of the four solutions. One can, however, underline two criteria that could lead to some preference for the Scenario II.

The first is the value of the chromomagnetic coupling κ_{cq}. We expect the fitted parameter to be close to the analogous parameter derived for the S-wave tetraquarks, which is $[\kappa_{cq}]_S \simeq 67$ MeV as discussed in [8]. Indeed, there are no reasons to believe that the chromomagnetic coupling κ_{cq} in the diquark should change with the addition of one unit of orbital angular momentum. At 95% C.L., the allowed value of κ_{cq} from the Y states in Scenario II (case 1) comes out somewhat smaller than anticipated, while it is somewhat larger in Scenario II (case 2). (See, the lower two frames in Fig. 2). Thus, this criterion would favor the Scenario SII.

A second expectation is for the Hamiltonian in Eq. (10) to describe both S and P-wave states, with the same value of the diquark mass. As commented in [8], Y_2, which in SII corresponds to $Y(4330)$, is in the same spin state as the $X(3872)$ except that there is a gap in mass between the two, which here is fully accounted by B_Q and by the spin-orbit interaction. If this is the case, one can derive the excitation energy of one unit of orbital

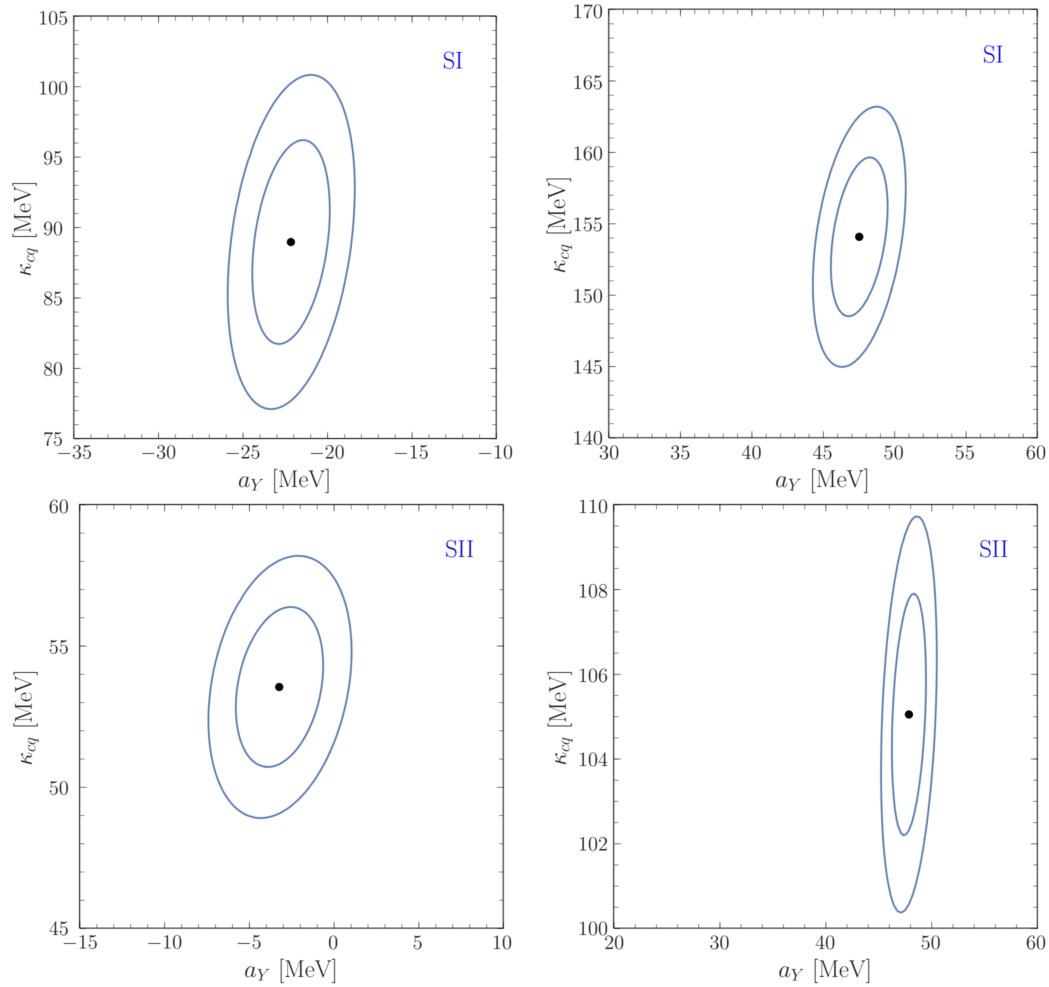

FIG. 2: 1σ- and 2σ-contours in the $a_Y - \kappa_{cq}$ parameter plane corresponding to 68.3% and 95.4% C.L. for the scenario I (SI) in the top two frames and scenario II (SII) in the bottom two frames. The dot in each frame shows the position of the best-fit value which is the minimum of the χ^2-function. The best-fit value of a_Y is negative (case 1) in the left panels and positive (case 2) in the right panels.

momentum from the equation

$$M_2 - M[X(3872)] = B_{\mathcal{Q}} - 2a_Y - [\kappa_{cq}]_P + [\kappa_{cq}]_S. \quad (21)$$

Using the input from Table III and $[\kappa_{cq}]_S = 67$ MeV, we obtain:

$$B_{\mathcal{Q}} = \begin{cases} 336 \text{ MeV} & \text{SI(c1)} \\ 545 \text{ MeV} & \text{SI(c2)} \\ 442 \text{ MeV} & \text{SII(c1)} \\ 596 \text{ MeV} & \text{SII(c2)} \end{cases} \quad (22)$$

However, if the diquark spin-spin coupling is fixed, say, $\kappa_{cq} = [\kappa_{cq}]_S = 67$ MeV, then the χ^2 analysis should be redone. In this case, there are four experimental input values and three unknown variables $\theta_k = (M_{00}, a_Y, b_Y)$. Thus, we have one degree of freedom and can discriminate minima according to $\chi^2_{\rm min}$. The best-fit values and variances of the parameters M_{00}, a_Y, and b_Y (all in MeV) corresponding to the minima with the lowest $\chi^2_{\rm min}$ in each scenario are reported in Table IV. There are other minima in both the scenarios, but their $\chi^2_{\rm min}$ are larger, and hence we don't discuss the resulting parameters. From this, one sees that with a fixed value $\kappa_{cq} = 67$ MeV, Scenario II is favored, having a good value of $\chi^2_{\rm min}$.

TABLE IV: Values of the parameters M_{00}, a_Y, b_Y (all in MeV), and $\chi^2_{\rm min}$/n.d.f. resulting from the χ^2 analysis with fixing $\kappa_{cq} = 67$ MeV.

Scenario	M_{00}	a_Y	b_Y	$\chi^2_{\rm min}$/n.d.f.
SI	4321 ± 79	2 ± 41	-141 ± 63	12.8/1
SII	4421 ± 6	22 ± 3	-136 ± 6	1.3/1

The values obtained for $B_{\mathcal{Q}}$ can be compared with the orbital angular momentum excitation energy in charmo-

TABLE V: First two columns: components of the eigenvector v_4 belonging to the highest eigenvalue, M_4, in the basis Y_3, Y_4. Third column, Probability of $S_{c\bar{c}} = 1$ in v_4.

	$Y_3,\ S=0$	$Y_4,\ S=2$	Prob.($S_{c\bar{c}}$=1) in v_4
SI (c1)	−0.27	0.96	0.94
SI (c2)	0.99	−0.03	0.25
SII(c1)	−0.58	0.82	0.75
SII (c2)	−0.95	0.30	0.32

nium, given by the analogous formula

$$B_Q = M(h_c) - \frac{1}{4}\left[3M(J/\psi) + M(\eta_c)\right] = 457 \text{ MeV}. \quad (23)$$

The combination of J/ψ- and η_c-meson masses eliminates the contribution of the S-wave spin-spin interaction in the J/ψ-meson, absent in the h_c, which has $S_{c\bar{c}} = 0$.

It is reasonable to believe that an $L = 1$ diquark-antidiquark system, with compact diquarks, is quite analogous to a $L = 1$ charmonium and, in that case, SlI(c1) is again favored.

The states with the masses M_3 and M_4 are linear combinations of the Y_3- and Y_4-states with the spins $S = 0$ and $S = 2$. We note that in both SI and SII, the eigenvectors corresponding to M_3 and M_4 in c1 are close to $S = 0$ and $S = 2$, respectively, while in c2, it is the opposite, *i.e.*, they are close to $S = 2$ and $S = 0$, respectively. Table V (column 1 and 2) gives the components of the eigenvector associated with M_4, which is called v_4, for different scenarios and solutions. The orthogonal vector v_3 is not shown. The eigenvectors carry interesting information; the projection of the eigenvector on the state with $c\bar{c}$ spin =1 is related to the probability of this state to decay into a J/ψ ($S_{c\bar{c}} = 1$) rather than in h_c ($S_{c\bar{c}} = 0$). The fourth column gives the probability of finding $S_{c\bar{c}} = 1$ in v_4. The table indicates that $Y(4660)$ in solutions c2 should have a good probability to decay into h_c while in c1 the J/ψ should dominate. This is quantified in the entries in Table V (third column).

Before concluding, we give the mass formula for the $L = 3$ state Y_5 in Table II. Including the tensor contribution, we get the following expression

$$M_5 - M_2 = 5B_Q - 14a_Y + 2\kappa_{cq} - \frac{8}{5}\,b_Y,$$
$$M_5 = \begin{cases} 6539 \text{ MeV} & \text{SI(c1)} \\ 6589 \text{ MeV} & \text{SI(c2)} \\ 6862 \text{ MeV} & \text{SII(c1)} \\ 6899 \text{ MeV} & \text{SII(c2)} \end{cases} \quad (24)$$

The values of B_Q are taken from (22) and the other parameters are from Table III. Without the b_Y term, Eq. (24) had been derived in [8] (with the opposite sign convention of a_Y).

V. CONCLUSIONS

We have derived the tensor contribution to the masses of the five $J^{PC} = 1^{--}$ tetraquarks Y_{1-5} using an effective Hamiltonian and correlating the parameters with those determined from the analysis of the five Ω_c states, which follows a similar approach. We find that the parameters are in the right ball-park, with the experimental Scenario II preferred. The current uncertainties on the masses of the Y-states hinder us to reach a completely quantitative conclusion. Hopefully, a clarification on the composition of Y states will be done at BESIII, Belle II, and LHCb. With precise measurements, parameters of the effective Hamiltonian can be determined more accurately, providing a quantitative test of the underlying diquark model.

Acknowledgements. We thank Marek Karliner, Sören Lange, Sheldon Stone, and Changzheng Yuan for helpful discussions. A.P. acknowledges partial support by the Russian Foundation for Basic Research (Project No. 15-02-06033-a). One of us (A.A.) would like to thank the CERN Physics Department for the hospitality, where this work originated. ADP thanks Ryan Mitchell and Alessandro Pilloni for informative discussions.

Appendix A: Spin-Orbit, Tensor Coupling and Wigner's 6j-Symbols

Combining three angular momenta, j_1, j_2, j_3 to a given J, one may follow two paths, characterized by the values of the intermediate angular momentum to which the first two are combined, *e.g.* j_1 and j_2 to j_{12} or j_2 and j_3 to j_{23}, each path corresponding to different base vectors. In the formulae given below, these two bases are characterized as follows

$$|(j_1, j_2)_{j_{12}}, j_3; J\rangle, \qquad |j_1, (j_2, j_3)_{j_{23}}; J\rangle, \quad (A1)$$

or, with a shorter notation

$$|j_{12}, j_3; J\rangle, \qquad |j_1, j_{23}; J\rangle, \quad (A2)$$

where it is understood that j_1, j_2, j_3 and J are held fixed.

Vectors in the two bases are, of course, related by a unitary transformation:

$$|j_1, j_{23}; J\rangle = \sum_{j_{12}} C_{j_{23}, j_{12}} |j_{12}, j_3; J\rangle. \quad (A3)$$

Besides j_{12} and j_{23}, the Clebsch-Gordon coefficients C depend upon the angular momenta that are being held fixed, j_1, j_2, j_3 and J, that is the Cs depend on *six angular momenta*. To maximize the symmetry properties, one rewrites (A3) as [28]:

$$|j_1, j_{23}; J\rangle = \sum_{j_{12}} (-1)^{j_1+j_2+j_3+J} \sqrt{(2j_{12}+1)(2j_{23}+1)} \times \begin{Bmatrix} j_1 & j_2 & j_{12} \\ j_3 & J & j_{23} \end{Bmatrix} |j_{12}, j_3; J\rangle. \quad (A4)$$

Wigner's $6j$-symbols are represented by the curly brackets. They appear in the calculation of the matrix elements of the spin-orbit Hamiltonian or the tensor coupling for two particles with spins S_1 and S_2 and different masses in the orbital angular momentum L. Examples are the P-wave Ω_c baryons and the diquark-antidiquark tetraquarks in P-wave, considered in the present paper.

In these cases, to classify states it is convenient to couple S_1 and S_2 to a total spin S and couple S to L to obtain the total J, that is:

$$j_1 = L, \quad j_2 = S_1, \quad j_3 = S_2, \quad j_{23} = S_1 + S_2 = S. \tag{A5}$$

In this basis the matrix elements of the total spin-orbit operator are easily computed according to the formula:

$$\boldsymbol{L} \cdot \boldsymbol{S} = \frac{1}{2}\left[J(J+1) - L(L+1) - S(S+1)\right]. \tag{A6}$$

In the spin-orbit interaction and in the tensor coupling, however, one encounters the matrix elements of the operator $\boldsymbol{L} \cdot \boldsymbol{S}_1 = \boldsymbol{j}_1 \cdot \boldsymbol{j}_2$, which would require a complicated calculation based on writing explicitly the states as products of three angular momentum states and applying the operator $\boldsymbol{L} \cdot \boldsymbol{S}_1$ to them.

A more convenient way to proceed is to use Eq. (A4) and set

$$j_1 = L, \quad j_2 = S_1, \quad j_{12} = L + S_1, \quad j_3 = S_2. \tag{A7}$$

In this basis,

$$\boldsymbol{L} \cdot \boldsymbol{S}_1 = \frac{1}{2}\left[j_{12}(j_{12}+1) - L(L+1) - S_1(S_1+1)\right], \tag{A8}$$

is diagonal on the basis vectors.

Using Eq. (A4), with Eq. (A5) on the lhs and Eq. (A7) on the rhs, one gets

$$\begin{aligned} &\boldsymbol{L} \cdot \boldsymbol{S}_1 |L, S; J\rangle \\ &= \sum_{j_{LS_1}} (-1)^{L+S_1+S_2+J} \sqrt{(2j_{LS_1}+1)(2S+1)} \\ &\times \frac{1}{2}\left[j_{LS_1}(j_{LS_1}+1) - L(L+1) - S_1(S_1+1)\right] \\ &\times \begin{Bmatrix} L & S_1 & j_{LS_1} \\ S_2 & J & S \end{Bmatrix} \; |j_{LS_1}, S_2; J\rangle. \end{aligned} \tag{A9}$$

Here, we have used the symbol $j_{12} = j_{LS_1}$, whereas $j_{23} = S$ on the lhs, according to (A5). It follows that:

$$\begin{aligned} &\langle L, S'; J|\boldsymbol{L} \cdot \boldsymbol{S}_1|L, S; J\rangle = \sqrt{(2S+1)(2S'+1)} \\ &\times \sum_{j_{LS_1}} \frac{1}{2}\left[j_{LS_1}(j_{LS_1}+1) - L(L+1) - S_1(S_1+1)\right] \\ &\times (2j_{LS_1}+1) \begin{Bmatrix} L & S_1 & j_{LS_1} \\ S_2 & J & S' \end{Bmatrix} \begin{Bmatrix} L & S_1 & j_{LS_1} \\ S_2 & J & S \end{Bmatrix}, \end{aligned} \tag{A10}$$

since by definition

$$\langle j_{12}, j_3; J|j_1, j_{23}; J\rangle = \langle j_1, j_{23}; J|j_{12}, j_3; J\rangle = C_{j_{23}, j_{12}}, \tag{A11}$$

is the coefficient given explicitly in Eq. (A4).

Tables of $6j$-symbols can be easily implemented in a computer code and they are already available, making use of the command `SixJSymbol[{`j_1, j_2, j_3`},{`j_4, j_5, j_6`}]`, in the symbolic computer algebra system Mathematica [29]. Therefore the result in (A10) can obtained with a program of a few lines [30]. In the following, we give the explicit formulae for the cases considered in the paper.

Ω_c baryons in P-wave. The constituents of the states are the $[ss]$-diquark and the charmed quark c with

$$j_1 = L = 1, \quad j_2 = S_{[ss]} = 1, \quad j_3 = S_c = 1/2. \tag{A12}$$

We will call $j_{12} = j_{LS_{[ss]}}$ and $j_{23} = S = 1/2, 3/2$. We have to consider the matrix $\boldsymbol{L} \cdot \boldsymbol{S}_{[ss]}$ in the two cases: $J = 1/2$ and $J = 3/2$. In the $J = 1/2$ case, $j_{LS_{[ss]}}$ can take the values $0, 1$ and Eq. (A10) reads:

$$\begin{aligned} &(\boldsymbol{L} \cdot \boldsymbol{S}_{[ss]})_{J=1/2} \equiv \langle 1, S'; 1/2|\boldsymbol{L} \cdot \boldsymbol{S}_{[ss]}|1, S; 1/2\rangle \\ &= \sqrt{(2S+1)(2S'+1)} \sum_{j_{LS_{[ss]}}=0}^{1} \left(2j_{LS_{[ss]}}+1\right) \\ &\times \frac{1}{2}\left[j_{LS_{[ss]}}(j_{LS_{[ss]}}+1) - 4\right] \\ &\times \begin{Bmatrix} 1 & 1 & j_{LS_{[ss]}} \\ 1/2 & 1/2 & S' \end{Bmatrix} \begin{Bmatrix} 1 & 1 & j_{LS_{[ss]}} \\ 1/2 & 1/2 & S \end{Bmatrix}, \end{aligned} \tag{A13}$$

where S, $S' = 1/2, 3/2$. This sum can be calculated easily when the required values of $6j$-symbols are known:

$$\begin{aligned} &\begin{Bmatrix} 1 & 1 & 0 \\ 1/2 & 1/2 & 1/2 \end{Bmatrix} = -\begin{Bmatrix} 1 & 1 & 0 \\ 1/2 & 1/2 & 3/2 \end{Bmatrix} = \frac{1}{\sqrt{6}}, \\ &\begin{Bmatrix} 1 & 1 & 1 \\ 1/2 & 1/2 & 1/2 \end{Bmatrix} = -\frac{1}{3}, \quad \begin{Bmatrix} 1 & 1 & 1 \\ 1/2 & 1/2 & 3/2 \end{Bmatrix} = -\frac{1}{6}. \end{aligned} \tag{A14}$$

Therefore, in the basis of states $({}^4P_{1/2}, {}^2P_{1/2})$ we have (the notation ${}^{2S+1}P_J$ is the same as in [21]):

$$(\boldsymbol{L} \cdot \boldsymbol{S}_{[ss]})_{J=1/2} = \begin{pmatrix} -5/3 & \sqrt{2}/3 \\ \sqrt{2}/3 & -4/3 \end{pmatrix}. \tag{A15}$$

In the same way

$$\begin{aligned} &(\boldsymbol{L} \cdot \boldsymbol{S}_{[ss]})_{J=3/2} \equiv \langle 1, S'; 3/2|\boldsymbol{L} \cdot \boldsymbol{S}_{[ss]}|1, S; 3/2\rangle \\ &= \sqrt{(2S+1)(2S'+1)} \sum_{j_{LS_{[ss]}}=1}^{2} \left(2j_{LS_{[ss]}}+1\right) \\ &\times \frac{1}{2}\left[j_{LS_{[ss]}}(j_{LS_{[ss]}}+1) - 4\right] \\ &\times \begin{Bmatrix} 1 & 1 & j_{LS_{[ss]}} \\ 1/2 & 3/2 & S' \end{Bmatrix} \begin{Bmatrix} 1 & 1 & j_{LS_{[ss]}} \\ 1/2 & 3/2 & S \end{Bmatrix}, \end{aligned} \tag{A16}$$

with the $6j$-symbol values:

$$\begin{aligned} &\begin{Bmatrix} 1 & 1 & 1 \\ 1/2 & 3/2 & 3/2 \end{Bmatrix} = \frac{\sqrt{10}}{12}, \quad \begin{Bmatrix} 1 & 1 & 2 \\ 1/2 & 3/2 & 1/2 \end{Bmatrix} = \frac{1}{2\sqrt{3}}, \\ &\begin{Bmatrix} 1 & 1 & 2 \\ 1/2 & 3/2 & 3/2 \end{Bmatrix} = \frac{1}{2\sqrt{30}}, \end{aligned} \tag{A17}$$

giving in the basis $({}^4P_{3/2},\ {}^2P_{3/2})$

$$(\boldsymbol{L}\cdot\boldsymbol{S}_{[ss]})_{J=3/2}=\begin{pmatrix}-2/3 & \sqrt{5}/3\\ \sqrt{5}/3 & 2/3\end{pmatrix}. \tag{A18}$$

Both results agree with [17].

Using the relation $(\boldsymbol{L}\cdot\boldsymbol{S}_c)=(\boldsymbol{L}\cdot\boldsymbol{S})-(\boldsymbol{L}\cdot\boldsymbol{S}_{[ss]})$, it is easy to get the matrices $(\boldsymbol{L}\cdot\boldsymbol{S}_c)_{J=1/2}$ and $(\boldsymbol{L}\cdot\boldsymbol{S}_c)_{J=3/2}$.

Diquarkonium in P-wave. The constituents are the $[cq]$ diquark and the $[\bar{c}\bar{q}']$ antidiquark.

$$j_1=L=1,\quad j_2=S_{[cq]}=1,\quad j_3=S_{[\bar{c}\bar{q}']}=1. \tag{A19}$$

Here, $J=1$ and $j_{23}=S=0,\ 1,\ 2$.

Note that the state with $S=1$ (and $L=1$) here has the charge conjugation C positive, opposite to the value of C of the other two states and of the Y states.

The spin-orbit coupling must be even under C and, therefore, it is represented by

$$\boldsymbol{L}\cdot(\boldsymbol{S}_{[cq]}+\boldsymbol{S}_{[\bar{c}\bar{q}']})=\boldsymbol{L}\cdot\boldsymbol{S}, \tag{A20}$$

which is diagonal on the states with $S=0,\ 2$.

However, the C-even combination of the spin-orbit couplings appearing in the tensor coupling is

$$(\boldsymbol{L}\cdot\boldsymbol{S}_{[cq]})^2+(\boldsymbol{L}\cdot\boldsymbol{S}_{[\bar{c}\bar{q}']})^2. \tag{A21}$$

Since $\boldsymbol{L}\cdot\boldsymbol{S}_{[cq]}$ is not C-invariant, it will mix the states with $S=0,2$ with the other state with $S=1$. Let us indicate with $|A\rangle$, $|B\rangle$ the states with $S=2,0$ and with $|C\rangle$ the state with $S=1$. In the square of, *e.g.* $\boldsymbol{L}\cdot\boldsymbol{S}_{[cq]}$, the state $|C\rangle$ appears as intermediate state, giving a contribution to both diagonal and non diagonal terms to the matrix elements of (A21) on $|A\rangle$ and $|B\rangle$

$$\langle i|(\boldsymbol{L}\cdot\boldsymbol{S}_{[cq]})^2|j\rangle+\langle i|(\boldsymbol{L}\cdot\boldsymbol{S}_{[\bar{c}\bar{q}']})^2|j\rangle \;=\; 2\langle i|\boldsymbol{L}\cdot\boldsymbol{S}_{[cq]}|C\rangle\times\langle C|\boldsymbol{L}\cdot\boldsymbol{S}_{[cq]}|j\rangle+\dots, \tag{A22}$$

where $i,\ j=A,\ B$.

In conclusion, we have to consider the full (3×3) matrix $\boldsymbol{L}\cdot\boldsymbol{S}_{[cq]}$. Using (A10) with definitions in (A19) we find:

$$\begin{aligned}(\boldsymbol{L}\cdot\boldsymbol{S}_{[cq]})_{J=1}&=\langle 1,S';1|\boldsymbol{L}\cdot\boldsymbol{S}_{[cq]}|1,S;1\rangle\\ &=\sqrt{(2S+1)(2S'+1)}\sum_{j_{LS_{[cq]}}=0}^{2}\left(2j_{LS_{[cq]}}+1\right)\\ &\times\frac{1}{2}\left[j_{LS_{[cq]}}(j_{LS_{[cq]}}+1)-4\right]\\ &\begin{Bmatrix}1 & 1 & j_{LS_{[cq]}}\\ 1 & 1 & S'\end{Bmatrix}\begin{Bmatrix}1 & 1 & j_{LS_{[cq]}}\\ 1 & 1 & S\end{Bmatrix},\end{aligned} \tag{A23}$$

where $S,\ S'=0,\ 1,\ 2$, obtaining (for $J=1$):

$$(\boldsymbol{L}\cdot\boldsymbol{S}_{[cq]})=\begin{pmatrix}-3/2 & 0 & 1/2\sqrt{5/3}\\ 0 & 0 & 2/\sqrt{3}\\ 1/2\sqrt{5/3} & 2/\sqrt{3} & -1/2\end{pmatrix}, \tag{A24}$$

in agreement with the result obtained with the direct method of applying the operators $\boldsymbol{L}\cdot\boldsymbol{S}_{[cq]}$ to the products of angular momentum vectors. Here, the following values of $6j$-symbols are required:

$$\begin{Bmatrix}1&1&0\\1&1&0\end{Bmatrix}=-\begin{Bmatrix}1&1&0\\1&1&1\end{Bmatrix}=\begin{Bmatrix}1&1&0\\1&1&2\end{Bmatrix}=\frac{1}{3}, \tag{A25}$$
$$\begin{Bmatrix}1&1&1\\1&1&1\end{Bmatrix}=\begin{Bmatrix}1&1&1\\1&1&2\end{Bmatrix}=\frac{1}{6},\quad \begin{Bmatrix}1&1&2\\1&1&2\end{Bmatrix}=\frac{1}{30},$$

and the rest can be obtained with the help of the $6j$-symbol symmetry under a permutation of columns and interchange of the upper and lower arguments in each of any two columns [28].

Using the relation $(\boldsymbol{L}\cdot\boldsymbol{S}_{[\bar{c}\bar{q}']})$=$(\boldsymbol{L}\cdot\boldsymbol{S})-(\boldsymbol{L}\cdot\boldsymbol{S}_{[cq]})$, we also get:

$$(\boldsymbol{L}\cdot\boldsymbol{S}_{[\bar{c}\bar{q}']})=\begin{pmatrix}-3/2 & 0 & -1/2\sqrt{5/3}\\ 0 & 0 & -2/\sqrt{3}\\ -1/2\sqrt{5/3} & -2/\sqrt{3} & -1/2\end{pmatrix}, \tag{A26}$$

again in agreement with the result obtained with the direct method.

Appendix B: Correlation Matrices

In this appendix the correlation matrices in the analysis of the data on Y states are collected. We label them in accordance with the notation used in Table III.

SI (c1):

$$R=\begin{pmatrix}1 & -0.890 & 0.995 & -0.990\\ & 1 & -0.888 & 0.896\\ & & 1 & -0.997\\ & & & 1\end{pmatrix}. \tag{B1}$$

SI (c2):

$$R=\begin{pmatrix}1 & -0.927 & 0.974 & -0.960\\ & 1 & -0.958 & 0.967\\ & & 1 & -0.996\\ & & & 1\end{pmatrix}. \tag{B2}$$

SII (c1):

$$R=\begin{pmatrix}1 & 0.971 & 0.986 & -0.968\\ & 1 & 0.970 & -0.952\\ & & 1 & -0.989\\ & & & 1\end{pmatrix}. \tag{B3}$$

SII (c2):

$$R=\begin{pmatrix}1 & 0.838 & -0.528 & 0.686\\ & 1 & -0.534 & 0.674\\ & & 1 & -0.972\\ & & & 1\end{pmatrix}. \tag{B4}$$

[1] A. Ali, J. S. Lange and S. Stone, arXiv:1706.00610 [hep-ph].
[2] A. Esposito, A. Pilloni and A. D. Polosa, Phys. Rept. **668**, 1 (2016).
[3] H. X. Chen, W. Chen, X. Liu and S. L. Zhu, Phys. Rept. **639**, 1 (2016).
[4] F. K. Guo, C. Hanhart, U. G. Meissner, Q. Wang, Q. Zhao and B. S. Zou, arXiv:1705.00141 [hep-ph].
[5] L. Maiani, F. Piccinini, A. D. Polosa and V. Riquer, Phys. Rev. D **71**, no. 1, 014028 (2005).
[6] A. Ali, C. Hambrock and W. Wang, Phys. Rev. D **85**, no. 5, 054011 (2012).
[7] R. L. Jaffe and F. Wilczek, Phys. Rev. Lett. **91**, no. 23, 232003 (2003).
[8] L. Maiani, F. Piccinini, A. D. Polosa and V. Riquer, Phys. Rev. D **89**, no. 11, 114010 (2014).
[9] M. Ablikim *et al.* [BESIII Collaboration], Phys. Rev. Lett. **118**, no. 9, 092001 (2017).
[10] G. Cotugno, R. Faccini, A. D. Polosa and C. Sabelli, Phys. Rev. Lett. **104**, no. 13, 132005 (2010).
[11] K. Abe *et al.* [Belle Collaboration], hep-ex/0612006.
[12] Q. Wang, C. Hanhart and Q. Zhao, Phys. Rev. Lett. **111**, no. 13, 132003 (2013).
[13] F. E. Close and P. R. Page, Phys. Lett. B **628**, 215 (2005).
[14] M. Ablikim *et al.* [BESIII Collaboration], Phys. Rev. Lett. **118**, no. 9, 092002 (2017).
[15] R. F. Lebed and A. D. Polosa, Phys. Rev. D **93**, no. 9, 094024 (2016).
[16] R. Aaij *et al.* [LHCb Collaboration], Phys. Rev. Lett. **118**, no. 18, 182001 (2017).
[17] M. Karliner and J. L. Rosner, Phys. Rev. D **95**, no. 11, 114012 (2017).
[18] W. Wang and R. L. Zhu, Phys. Rev. D **96**, no. 1, 014024 (2017).
[19] M. Padmanath and N. Mathur, Phys. Rev. Lett. **119**, no. 4, 042001 (2017).
[20] T. M. Aliev, S. Bilmis and M. Savci, arXiv:1704.03439 [hep-ph].
[21] M. Karliner and J. L. Rosner, Phys. Rev. D **92**, no. 7, 074026 (2015).
[22] L. D. Landau and E. M. Lifshitz, *Quantum Mechanics (Nonrelativistic Theory)*, 3rd edition. (Pergamon Press, Oxford, 1977), p. 96.
[23] D. Ebert, R. N. Faustov, V. O. Galkin and A. P. Martynenko, Phys. Rev. D **66**, no. 1, 014008 (2002).
[24] A. Ali, I. Ahmed, M. J. Aslam and A. Rehman, Phys. Rev. D **94**, no. 5, 054001 (2016).
[25] N. V. Drenska, R. Faccini and A. D. Polosa, Phys. Lett. B **669**, 160 (2008).
[26] C. Patrignani *et al.* [Particle Data Group], Chin. Phys. C **40**, no. 10, 100001 (2016).
[27] X. Y. Gao, C. P. Shen and C. Z. Yuan, Phys. Rev. D **95**, no. 9, 092007 (2017).
[28] A. R. Edmonds, *Angular Momentum in Quantum Mechanics.* (Princeton University Press, Princeton, New Jersey, 1957).
[29] Wolfram Research, Inc., Mathematica, Version 11.1, Champaign, IL (2017).
[30] W. J. Thompson, *Angular Momentum: An Illustrated Guide to Rotational Symmetries for Physical Systems.* (Wiley-VCH, Weinheim, 2004).